


RESEARCH

Open Access



# IFN- $\alpha$ and vitamin B6-induced galectin-9 promotes the immunomodulatory function of human clonal mesenchymal stem cells

Jee-Hoon Nam<sup>1,2†</sup>, Jeong Hyun Moon<sup>1,2†</sup>, Byeol Choi<sup>2</sup>, Geun-Hyung Kang<sup>2</sup>, Yunok Park<sup>2</sup>, Se-Yeon Park<sup>2</sup>, Tae-Hyun Ko<sup>2</sup>, Donghee Shin<sup>2</sup>, YoungSu Jung<sup>2</sup>, Si-Na Kim<sup>2</sup>, Yun-Kyoung Cho<sup>2</sup> and Myung-Shin Jeon<sup>1,2,3,4\*</sup> 

## Abstract

**Background** Mesenchymal stem cells (MSCs) possess a variety of immunomodulatory functions that can vary depending on the MSC line. Investigating priming strategies is essential for increasing the immunomodulatory potential of MSCs.

**Methods** Human clonal MSCs (cMSCs) were primed with TNF- $\alpha$ , IFN- $\gamma$ , IL-1 $\beta$ , IFN- $\alpha$ , and vitamin B6. Their immunomodulatory functions, including T-cell proliferation and cytokine production, were analyzed. The primed cMSCs were injected intravenously into a mouse model of ovalbumin-induced atopic dermatitis (AD), and their therapeutic effects were evaluated.

**Results** We identified IFN- $\alpha$  and vitamin B6 as promising priming agents when they are combined with TNF- $\alpha$  and IFN- $\gamma$ . The primed cMSCs showed expression of galectin-9 (Gal-9), IL-1Ra, and PDL-1. Gal-9 facilitates the induction of regulatory T cells (Tregs) and apoptosis. Treatment with primed cMSCs significantly alleviated pathological changes in an AD mouse model. Notable improvements included a reduction in epidermal thickness ( $p < 0.05$ ), a decreased number of mast cells and eosinophils in the dermis ( $p < 0.01$ ), restored expression of claudin-1 in the epidermis ( $p < 0.0001$ ), and lower serum levels of IgE ( $p < 0.05$ ).

**Conclusions** This novel combination of priming factors significantly promotes the immunomodulatory functions of cMSCs by inducing Gal-9. Consequently, Gal-9 may serve as an excellent biomarker for screening primed cMSCs for their immunomodulatory capabilities, facilitating a more accurate assessment of their therapeutic effectiveness.

**Keywords** Atopic dermatitis, Clonal mesenchymal stem cell, Galectin-9, IFN- $\alpha$ , Priming, Vitamin B6

<sup>†</sup>Jee-Hoon Nam and Jeong Hyun Moon have contributed equally to this work.

\*Correspondence:  
Myung-Shin Jeon  
msjeon@inha.ac.kr

<sup>1</sup> Department of Molecular Biomedicine, College of Medicine, Inha University, Incheon, Republic of Korea

<sup>2</sup> Research Institute, SCM Lifescience, Incheon, Republic of Korea

<sup>3</sup> Translational Research Center, Inha University School of Medicine, Inha University Hospital, B/308 Jungseok Bldg., 366 Seohae-Daero, Jung-Gu, Incheon 22332, Republic of Korea

<sup>4</sup> Program in Biomedical Science & Engineering, Inha University, Incheon, Republic of Korea

## Background

Mesenchymal stem cells (MSCs) modulate the innate and adaptive immune systems primarily through the secretion of cytokines, chemokines, and growth factors and through direct interactions with immune cells [1, 2]. MSCs represent a promising cell-based therapy for clinical applications in treating inflammatory diseases, including graft-versus-host disease (GVHD), asthma, Crohn's disease, and atopic dermatitis (AD), owing to their anti-inflammatory, immunosuppressive, immunomodulatory, and regenerative properties [3–6]. Given the heterogeneity of the immunomodulatory profiles of MSCs, we



previously developed a subfractionation culture method (SCM) to isolate clonal MSCs (cMSCs) from human bone marrow [7–9]. This method allows us to separate distinct cMSC lines that exhibit notable variations in their immunomodulatory capabilities. Some cMSCs possess strong immunomodulatory functions, whereas others exhibit limited capabilities [10].

Increasing the efficacy of cMSCs with low immunomodulatory ability is essential for improving the efficacy of clinical trials. We aimed to promote the functionality of cMSCs by priming them in inflammatory environments that mimic disease conditions. This priming process is crucial for optimizing the efficacy of MSC-based therapies, which have shown promise in treating various diseases. Various priming techniques have been developed, including pro-inflammatory cytokines, growth factors, pharmacological or chemical agents, hypoxic conditions, and three-dimensional (3D) culture environments [11–14]. Among these, cytokines have been shown to increase the immunosuppressive and immunomodulatory functions of MSCs more effectively than other approaches. Among the various cytokines, MSCs stimulated with a combination of TNF- $\alpha$  and IFN- $\gamma$  (T/I) exhibit the most significant improvement in immunomodulatory capacity [15]. Notably, the expression of immunosuppressive molecules, including indoleamine 2,3-dioxygenase (IDO), prostaglandin E2 (PGE2), intracellular adhesion molecule-1 (ICAM-1), and galectin-9 (Gal-9), is upregulated [16–20]. Furthermore, these primed MSCs promote the expression of immune checkpoints such as programmed death ligand-1 (PD-1) and CTLA-4 on T cells, further diminishing their activity [15, 17, 20, 21]. IFN- $\alpha$  has been used to treat various tumors, including leukemia, melanoma, and lymphoma, due to its ability to inhibit cell proliferation, restrict tumor angiogenesis, and induce apoptosis [22–24]. IFN- $\alpha$ -overexpressing mouse MSCs effectively suppressed tumor growth via infiltrating CD8<sup>+</sup> T cells and even stronger anti-tumor immunity in combination with PD-L1 blockade [25]. MSCs express PD-L1 on their surface, and interacting with PD-1 on T cells inhibits T cell activation, proliferation, and cytokine secretion, thereby contributing to an immunosuppressive environment [26].

MSCs are exposed to oxidative and nitrosative stress due to elevated levels of reactive oxygen species (ROS) and reactive nitrogen species (RNS) during in vitro expansion and after in vivo transplantation, potentially compromising their function and viability [27]. Vitamins, such as vitamin C and E, can serve as effective antioxidants [27, 28]. Antioxidant supplementation has been shown to increase cell survival, promote proliferation, and inhibit senescence in MSCs [27, 29]. Adipose-derived MSCs preconditioned with pyridoxal-5'-phosphate

(PLP), the active form of vitamin B6, significantly inhibited T cell proliferation [30].

Thus, this study aimed to investigate the potential promotion of AD alleviation by priming weak immunomodulatory MSCs with a combination of cytokines and vitamins.

## Methods

### cMSC culture and priming of cMSCs

Bone marrow-derived cMSCs were used in this study. Bone marrow samples were obtained from five healthy donors. One sample was purchased from AllCells (Alameda, CA, USA), while the other four were donated by the Catholic University of Korea, Seoul St. Mary's Hospital. Informed consent was obtained from all participants, and all procedures were approved by the Institutional Review Board (IRB) of the Catholic University of Korea, Seoul St. Mary's Hospital (IRB No. KC15CSSE0336) and AllCells (IRB No. 949–542–3882).

Clonal MSCs (cMSCs) were isolated from bone marrow via a subfractionation method [8]. This technique involves multiple transfers of bone marrow culture supernatants, facilitating the separation of single-cell-derived MSC colonies [8]. cMSCs were seeded at a density of  $0.26 \times 10^6$  cells per 175 T flask (Nunc, Roskilde, Denmark) in MEM-alpha medium. After 6 days, approximately  $2$  to  $3 \times 10^6$  cMSCs were harvested. The cMSCs were then reseeded at a density of  $1.1 \times 10^6$  cells per 75 T flask (Nunc) for priming. The following day, the cMSCs were primed for 24 h under the following stimulation conditions: 20 ng/mL IL-1 $\beta$  (R&D Systems, Minneapolis, MN, USA), 20 ng/mL IFN- $\alpha$  (Abcam, Cambridge, UK), 50  $\mu$ g/mL vitamin B6 (Sigma-Aldrich, St. Louis, MO, USA), 10 ng/mL TNF- $\alpha$  (R&D Systems), and 10 ng/mL IFN- $\gamma$  (BD Biosciences, Franklin Lakes, NJ, USA). pcMSC1 cells were primed with a combination of IFN- $\alpha$  and vitamin B6, along with IL-1 $\beta$ . T/I cMSCs were primed with TNF- $\alpha$  and IFN- $\gamma$  (T/I), while pcMSC2 were primed with IFN- $\alpha$  and vitamin B6, in addition to T/I.

All MEM-alpha media contained 4% human platelet lysate (hPL; Mill Creek Life Sciences, Rochester, MN, USA) as a substitute for fetal bovine serum, 20  $\mu$ g/mL gentamicin (Gibco), and 0.25 $\times$  mycoplasma elimination reagent (MycoZap<sup>TM</sup> Prophylactic, Lonza, Rockville, MD, USA) to prevent potential bacterial and mycoplasma contamination during cell passaging. The hPL from Mill Creek Life Sciences was pretreated with an anticoagulant, so no additional heparin was added during cell culture.

Cell surface expression of PD-L1 (BD Biosciences) and intracellular proteins of IL-1Ra (Invitrogen, Carlsbad, CA, USA) and Gal-9 (Biolegend, San Diego, CA, USA) were analyzed using the BD FACS Verse<sup>TM</sup> instrument. Intracellular proteins were stained using the

Cytofix/Cytoperm™ Fixation/Permeabilization Kit (BD Biosciences) according to the manufacturer's instructions. The data were analyzed using FlowJo software (BD Biosciences). All antibodies were obtained from BD Biosciences.

#### Quantitative reverse transcription–polymerase chain reaction (qRT-PCR) and RNA sequencing analysis

mRNA was isolated from cMSCs via a MiniBEST RNA extraction kit (TaKaRa, Shiga, Japan), and cDNA was synthesized with the PrimeScript™ RT Reagent Kit (TaKaRa) according to the manufacturer's instructions. The cDNA products were amplified using TB Green Premix EX Taq™ (TaKaRa) and analyzed via a StepOnePlus Real-Time PCR System (Applied Biosystems, Waltham, MA, USA). The target genes for qRT-PCR were as follows. *ICOSLG* (Inducible T-cell Costimulator Ligand), *IDO1* (Indoleamine 2,3-Dioxygenase 1), *PTGS2* (Prostaglandin-Endoperoxide Synthase 2, also known as TSG-6), *LGALS9* (Galectin-9), *IL1RN* (Interleukin-1 Receptor Antagonist), *IL6* (Interleukin-6), *CD274* (Programmed Death-Ligand 1, PD-L1), *PDCD1LG2* (Programmed Death-Ligand 2, PD-L2), *VCAM1* (Vascular Cell Adhesion Molecule 1), *ICAM1* (Intercellular Adhesion Molecule 1), *EGF* (Epidermal Growth Factor), *HGF* (Hepatocyte Growth Factor), *VEGFA* (Vascular Endothelial Growth Factor A), *LGALS1* (Galectin-1), *TGFB1* (Transforming Growth Factor Beta 1), *CXCL12* (C-X-C Motif Chemokine Ligand 12), *CXCL1* (C-X-C Motif Chemokine Ligand 1), *CCL7* (C-C Motif Chemokine Ligand 7), *MDK* (Midkine), *IL4* (Interleukin-4), *IL5* (Interleukin-5), *IL13* (Interleukin-13), *CD8A* (CD8 Alpha Chain). All primers were supplied by QIAGEN (Hilden, Germany), which does not disclose the sequences of the primers. The PCR conditions included an initial hot start at 95 °C for 5 min to activate the DNA polymerase, followed by cycling at 95 °C for 15 s and 60 °C for 1 min for 40 cycles.

Total RNA from harvested pcMSCs was sent to eBioGen (Seoul, Republic of Korea) for RNA sequencing analysis using QuantSeq 3' mRNA-Seq. Before RNA sequencing, quality control processes were performed to evaluate RNA quality. The results were analyzed using ExDEGA and ExDEGA GraphicPlus tools provided by eBioGen (Seoul, Republic of Korea).

#### Coculture of PBMCs and pcMSCs under PHA-stimulated conditions

Blood samples were collected from healthy donors to isolate peripheral blood mononuclear cells (PBMCs). Informed consent was obtained from all participants, and all procedures were approved by the Institutional Review Board (IRB) of Inha University Hospital (IRB No. 10–51).

T-cell proliferation was analyzed using carboxyfluorescein succinimidyl ester (CFSE; Invitrogen). CFSE-stained PBMCs were cultured with pcMSCs at a 10:1 ratio. A total of  $1 \times 10^6$  PBMCs were stimulated with 5 µg/mL phytohemagglutinin (PHA; Sigma–Aldrich) in the presence of  $1 \times 10^5$  pcMSCs in 1 mL of medium (HyClone, Cytiva, Logan, UT, USA) in a 24-well plate. After 4 days, CD3<sup>+</sup> T cells were identified using anti-CD3-PE (OKT3, BioLegend), and both CFSE-positive and CFSE-negative T cells were analyzed using flow cytometry (BD FACSVerse, BD Biosciences) and FlowJo software (BD Biosciences). The supernatants collected for ELISAs were stored at –80 °C in a storage box and used within 10 days. With an ELISA kit, the levels of human IFN-γ, TNF-α, IL-2, IL-5, IL-10, IL-17A (R&D Systems), and galectin-9 (Abcam) in the supernatants were quantified with a Synergy H1 Multimode Reader (Agilent BioTek, Santa Clara, CA, USA). The optical density (O.D.) range of the microplate reader was 0–4.0.

#### Differentiation of regulatory T cells and Th17 cells

For the differentiation of regulatory T cells (Tregs), CD4 T cells were isolated from PBMCs via a CD4 T cell isolation kit (STEMCELL, Vancouver, Canada) according to the manufacturer's instructions. The wells of a 48-well plate were coated overnight at 4 °C with 500 µL of a 1 µg/mL solution of anti-CD3 (OKT3, Invitrogen). Purified CD4 T cells ( $5 \times 10^5$ ) were stimulated for 2 days with 3 µg/mL anti-CD28 (CD28.2, Invitrogen) antibodies, 1 ng/mL IL-2, 5 ng/mL TGF-β (R&D Systems), and 0.1 µM of all-trans retinoic acid (Sigma–Aldrich) in the presence or absence of pcMSCs ( $5 \times 10^4$  cells/well) [31]. The cells were stained for CD4, CD25, and FOXP3 using the Transcription Factor Fixation/Permeabilization Concentrate and Diluent Kit (Invitrogen) and analyzed by flow cytometry. For induction of Th17 differentiation [32, 33], the wells of a 96-well plate were coated overnight at 4 °C with 200 µL of a 1 µg/mL solution of anti-CD3 (OKT3; Invitrogen). CD4 T cells ( $2 \times 10^5$ ) were stimulated with 1 µg/mL anti-CD28 (CD28.2; Invitrogen), 20 ng/mL IL-23 (R&D Systems), and 20 ng/mL IL-1β (R&D Systems) in the presence or absence of pcMSCs ( $5 \times 10^4$  cells/well). After 7 days, the concentration of IL-17A in the supernatant was analyzed via ELISAs. For neutralization, 4 µg/mL anti-PD-L1 (R&D Systems), 5 µg/mL anti-galectin-9 (BioLegend), or 10 µg/mL anti-IL-1Ra (R&D Systems) was added to the culture media.

#### Measurement and analysis of T-cell apoptosis induction

PBMCs ( $1 \times 10^6$ ) were cocultured with pcMSCs ( $1 \times 10^5$ ) at a 10:1 ratio in a 24-well plate under stimulation conditions with 1 µg/mL soluble anti-CD3 (OKT3, Invitrogen) and 1 µg/mL soluble anti-CD28 (CD28.2,

Invitrogen). After 72 h, the harvested cells were stained with a CD4 antibody (RPA-T4, Invitrogen), washed, and finally stained with Annexin V/propidium iodide (PI) in Annexin V buffer (BD Biosciences). An apoptosis detection kit (BD Biosciences) was used according to the manufacturer's instructions. Apoptotic CD4<sup>+</sup> T cells were immediately analyzed by flow cytometry.

### AD animal model

The work has been reported in line with the ARRIVE guidelines 2.0. The animals used in this experiment were six-week-old female and specific pathogen-free BALB/c mice, each weighing between 15 and 20 g. The animals were supplied by Orient Bio (Seongnam, Republic of Korea). The experiment commenced following a 5 days acclimation period in the animal facility, a crucial step to ensure that the mice adapted to their new environment and to reduce stress. The housing conditions at the Center for Animal Care and Use (CACU) at Gachon University Gil Medical Center included a temperature range of 22–25 °C, humidity levels between 40 and 60%, and a 12 h light–dark cycle from 7:00 to 19:00. The mice were housed in groups of five in cages under lighting conditions of 150 to 300 lx, with ad libitum access to sterile distilled water and solid feed. The study was designed and conducted according to the regulations of the Institutional Animal Care and Use Committee (IACUC) of Gachon University (IACUC No. LCDI-2023–0054).

AD was induced as previously described with modifications [34, 35]. Seven-week-old female BALB/c mice were immunized with 10 µg of ovalbumin (grade V; Sigma–Aldrich), mixed with 4 mg of aluminum hydroxide as an adjuvant (Thermo Fisher Scientific, Waltham, MA, USA), in a total volume of 200 µL. This mixture was administered three times at one-week intervals (on Days 0, 7, and 14), with two doses given intraperitoneally and one administered subcutaneously. On Day 21, the mice were sensitized epicutaneously using ovalbumin (OVA) patches. Each patch contained 60 µg of OVA prepared

in 60 µL of PBS and was made from a 1.2×1.2 cm piece of sterile gauze. The patch was applied to the shaved backs of the mice and secured to the skin with a transparent dressing (Tegaderm™; 3 M, St. Paul, MN, USA). The patches were changed two to three times per week, ensuring that the skin remained in contact with the OVA for 10 days. On Day 30, blood sera were collected to measure IgE levels (BD Biosciences), an AD marker, via an ELISA kit (BD Biosciences). The mice induced with AD (n=60) were randomly assigned to groups based on their IgE levels (Supplementary Fig. S1). Mice whose IgE levels were significantly lower or higher than average were excluded from the study. The IgE levels were comparable across all the AD-induced groups (n=10 per group). Several mice died during the experiment, resulting in the following final counts for each group: naive (n=5), vehicle (n=9, PBS), Group 1 (n=10, nonprimed cMSCs), Group 2 (n=9, pcMSC1), Group 3 (n=8, T/I-primed cMSCs), and Group 4 (n=10, pcMSC2). cMSCs (3.3×10<sup>5</sup> cells) in 200 µL of PBS were intravenously injected into the mice on Days 42, 44, and 49. The skin was subsequently re-exposed to OVA for 10 days. On Day 59, all the animals were euthanized using inhaled isoflurane (Kyungbo Pharmaceutical Co., Ltd., Asan, Republic of Korea) anesthesia. Sera and skin biopsy samples were obtained for ELISA and histological examination, respectively [36]. As described above, the overall process for inducing the AD model is summarized as a graphical schematic in Fig. 1. Mouse IgG1 and IgG2a serum levels were measured using ELISA kits (Abcam).

### Histopathology

Skin tissue from each mouse was harvested and fixed in 10% formalin (Sigma–Aldrich) for 24 h at room temperature (RT). The tissues were dehydrated through a graded series of ethanol (70%, 80%, 90%, and 100%) and xylene, then embedded in paraffin. The tissues were sectioned to a thickness of 3 µm using a microtome (Microm HM 355, Epreidia, Kalamazoo, MI, USA). For staining, the

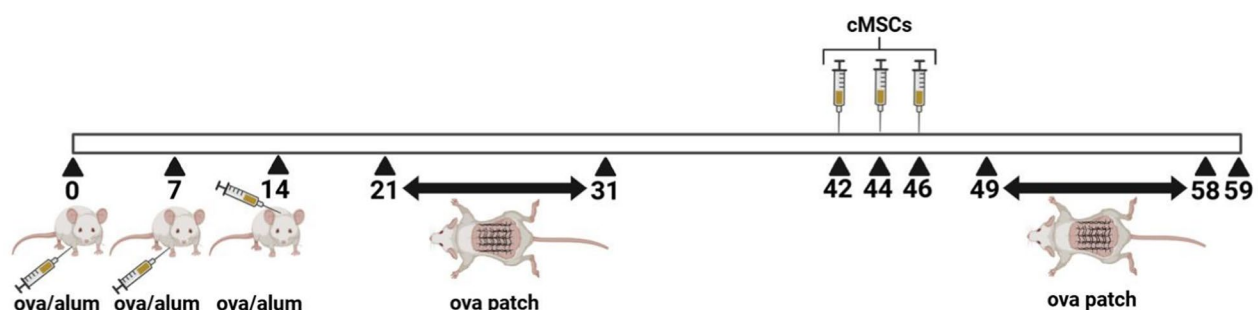


**Fig. 1** Graphical schematic for the AD model. A schematic diagram illustrating the cMSC injection process following the induction of AD in a mouse model



sections were deparaffinized by incubation at 60 °C for 1 h, followed by three washes in 100% xylene, each lasting 5 min. The sections were rehydrated through a graded series of ethanol (100%, 90%, 80%, and 70%) and rinsed with tap water.

The tissue sections were incubated in 10 mM Tris–EDTA buffer (pH 9.0) for antigen retrieval and subsequently heated in a microwave at a boiling temperature for 3 min. After heating, the sections were allowed to cool to room temperature (RT) for 1 h. The sections were washed three times with tap water following the cooling period. For blocking of nonspecific binding, the sections were incubated with Protein Block (Cat. No. X0909, Dako, Glostrup, Denmark) at RT for 10 min, after which the blocking solution was removed without further washing. Claudin-1 (CLDN1) expression was analyzed through immunofluorescence (IF) staining. The CLDN1 primary antibody (MH25; Thermo Fisher Scientific) was diluted 1:500 in Antibody Diluent (Cat. No. S3022, Dako) and incubated at room temperature for one hour in a humidified chamber. After three washes with TBST, the sections were incubated with Alexa Fluor Texas Red-conjugated goat anti-rabbit IgG (T2767; Invitrogen) diluted 1:1000 in antibody diluent for one hour at room temperature in a humidified chamber. Following another set of three TBST washes, the nuclei were counterstained with VECTASHIELD Antifade Mounting Medium with DAPI (Vector Laboratories, CA, USA). CLDN1 expression after IF staining was analyzed using the Lionheart FX system (Agilent BioTek), and the mean fluorescence intensity (MFI) per unit area was measured in the epidermal layer.

Hematoxylin and eosin (H&E) staining was performed to assess the lengths of the epidermis and dermis. Additionally, toluidine blue (Sigma–Aldrich) staining was used to evaluate mast cell infiltration into the dermis, whereas Congo red (Sigma–Aldrich) staining was used to quantify eosinophils. The stained slides were scanned using the Panoramic SCAN II system (3DHitech Ltd., Budapest, Hungary) and analyzed with CaseViewer software (3DHitech Ltd.). Skin thickness analysis was conducted on H&E-stained photographs of individual mouse skin at 100× magnification. Dermal thickness was defined as the distance from the epidermal-dermal junction to the adipose tissue of the hypodermis, whereas epidermal thickness was defined as the distance from the epidermal-dermal junction to the stratum corneum. Five thickness measurements were taken per slide, and the pixel-based thickness measurements were converted to micrometers. Mast cells and eosinophils were counted from three randomly selected fields per slide, with two slides examined per mouse. The three fields were initially identified by scanning the entire slide at 100× magnification. Positively

stained cells were counted in a high-power field (HPF) at 200× magnification.

### Statistical analysis

All the data were statistically analyzed using GraphPad Prism version 8.4.3 (California, CA, USA). Most statistical *p* values were evaluated using one-way analysis of variance (ANOVA). A *t* test was conducted to compare the two groups, and Tukey's HSD post hoc test was applied when appropriate.

## Results

### Different immunomodulatory functions of cMSCs isolated from various donors

The immunomodulatory effects of the five cMSCs were evaluated by measuring T-cell proliferation and cytokine production. The inhibitory effects on T-cell proliferation and IFN- $\gamma$  production varied among the different cMSCs. At a 10:1 ratio, the immunomodulatory functions were reduced compared with those at a 5:1 ratio (Fig. 2). Notably, cMSC1 exhibited the lowest immunomodulatory capacity among the five cMSCs.

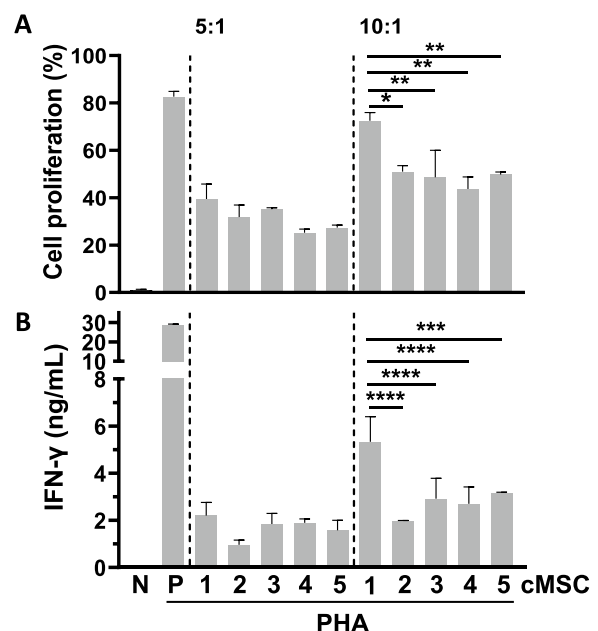


**Fig. 2** Diversity of the immunomodulatory capacities of various cMSCs. **A** Flow cytometry analysis of T-cell proliferation. **B** IFN- $\gamma$  levels measured by ELISA. N: negative control, P: positive control. The error bars indicate the standard deviation (SD). Two independent experiments were conducted. \**p* values were determined using one-way ANOVA. Significance levels: \**p* < 0.05, \*\**p* < 0.01, and \*\*\*\**p* < 0.0001

### Promotion of the immunomodulatory properties of cMSCs through various combinations of priming factors

Our research revealed promising opportunities to enhance the immunomodulatory capacity of cMSCs. We used cMSC1, which exhibited the lowest immunomodulatory capacity (Fig. 2), to screen a variety of cytokines, including IL-2, IL-6, and IFN- $\alpha$ , along with a selection of vitamins, such as vitamin B6, to optimize the immunomodulatory functions of cMSC1 (data not shown). We identified IFN- $\alpha$  and Vit B6 as effective agents. These factors combine with either IL-1 $\beta$  or TNF- $\alpha$  and IFN- $\gamma$  (T/I), resulting in two primed cell types: pcMSC1 (IL-1 $\beta$ , IFN- $\alpha$ , and Vit B6) and pcMSC2 (T/I, IFN- $\alpha$ , and Vit B6).

The mRNA expression levels of ICOSL ( $p=0.0029$ ), IDO ( $p=0.0465$ ), TSG6 ( $p<0.0001$ ), IL-1Ra ( $p=0.013$ ), PD-L1 ( $p=0.0025$ ), ICAM-1 ( $p=0.0004$ ), and VCAM-1 ( $p=0.0011$ ) were significantly elevated in T/I-primed cMSCs compared to those with stimulation with IFN- $\gamma$  alone. Furthermore, compared with T/I-primed cMSCs (T/I), pcMSC2 exhibited an additional increase in TSG6 ( $p=0.0027$ ), Gal-9 ( $p=0.0177$ ), and IL-1Ra ( $p<0.0001$ ) levels (Fig. 3A). Priming factors did not affect the EGF, HGF, VEGF, Gal-1, TGF- $\beta$ 1, or CXCL12 levels; however, IL-1 $\beta$  and TNF- $\alpha$  significantly elevated CXCL1 levels (Supplementary Fig. S2).

We evaluated the immunomodulatory functions of cMSCs under specific priming conditions by coculturing the primed cMSCs with CFSE-stained PBMCs stimulated with PHA. Compared to non-primed cMSCs, primed cMSCs significantly inhibited cell proliferation and the secretion of IFN- $\gamma$  and TNF- $\alpha$ . Notably, T/I-primed cMSCs (T/I) and pcMSC2 effectively suppressed cell proliferation and the secretion of IFN- $\gamma$ , TNF- $\alpha$ , IL-5, and IL-17 ( $p<0.0001$ ) (Fig. 3B–F). Since Th2 cytokine levels are low in human PBMCs, we used mouse splenocytes stimulated with anti-CD3 and anti-CD28 antibodies in the presence of pcMSCs. Consistent with the findings observed in human PBMCs, the IFN- $\gamma$  and IL-17A levels were significantly reduced, whereas the IL-2 levels were increased in the presence of pcMSC2 ( $p<0.0001$ ). In addition, the levels of Th2 cytokines, including IL-4 and IL-13, were significantly decreased by pcMSC2 ( $p<0.0001$ ) (Supplementary Fig. S3). These findings indicate that priming with IFN- $\alpha$

and Vit B6 with T/I markedly increased the immunomodulatory capacity of cMSCs.

### pcMSC2 retains the characteristics of cMSCs

The characteristics of pcMSC2 were evaluated through various in vitro assays to determine whether they were maintained. Microscopic observation revealed that compared with nonprimed cMSCs, pcMSC2 retained their morphology and did not lose their ability to differentiate into adipocytes, osteocytes, or chondrocytes (Supplementary Fig. S4A and B). Additionally, during serial passaging, cell viability, PDL, and PDT remained at similar levels (Supplementary Fig. S4C). Furthermore, karyotype analysis confirmed that pcMSC2 did not exhibit genetic abnormality, and a soft agar colony formation assay demonstrated that pcMSC2 did not have tumorigenic potential (Supplementary Fig. S4D and E). Additionally, pcMSC2 were analyzed using flow cytometry to assess the expression of MSC-positive markers (CD44, CD73, CD90, CD105) and MSC-negative markers (CD14, CD31, CD34, CD45). All the markers were expressed at levels comparable to those of nonprimed cMSCs (Supplementary Table 2). Collectively, these findings indicate that pcMSC2 retained the fundamental characteristics of cMSCs.

### Induction of Gal-9 by priming

We observed a significant increase in the mRNA expression levels of PD-L1, IL-1Ra, and Gal-9 following priming (Fig. 3). Consistently, we noted elevated protein expression levels of these markers in T/I-primed cMSCs compared with those in nonprimed cMSCs (PD-L1:  $p<0.0001$ , IL-1Ra:  $p<0.0001$ , Gal-9:  $p=0.0109$ ). Furthermore, in pcMSC2 cells, the protein expression levels of IL-1Ra and Gal-9 were markedly greater than those in T/I-primed cMSCs (IL-1Ra:  $p=0.003$ , Gal-9:  $p=0.0053$ ) (Fig. 4A). These findings suggest that the combination of IFN- $\alpha$  and Vit B6 increases the expression of IL-1Ra and Gal-9 in pcMSC2.

To further investigate the individual effects of IFN- $\alpha$  and Vit B6, we primed cMSC1 with IFN- $\alpha$  and Vit B6 separately, in addition to the T/I combination, and conducted RNA sequencing analysis. The results indicated that the expression of this gene was significantly different from that in T/I-primed cMSCs (Fig. 4B, Supplementary

(See figure on next page.)

**Fig. 3** Screening of priming conditions to promote the immunomodulatory functions of cMSCs. **A** Expression of immunomodulatory genes in cMSCs after treatment with various cytokines and vitamin B6. **B** T-cell proliferation by flow cytometry. **C–F** IFN- $\gamma$ , TNF- $\alpha$ , IL-5, and IL-17A levels measured by ELISA. Error bars represent standard deviation (SD). \* $p$  and # $p$  values represent comparisons with nonprimed and T/I-stimulated cMSCs, respectively. All  $p$  values were determined using one-way ANOVA. Significance levels: \* $p<0.05$ , \*\* $p<0.01$ , \*\*\* $p<0.001$ , \*\*\*\* $p<0.0001$ , # $p<0.05$ , ## $p<0.01$ , and ### $p<0.001$

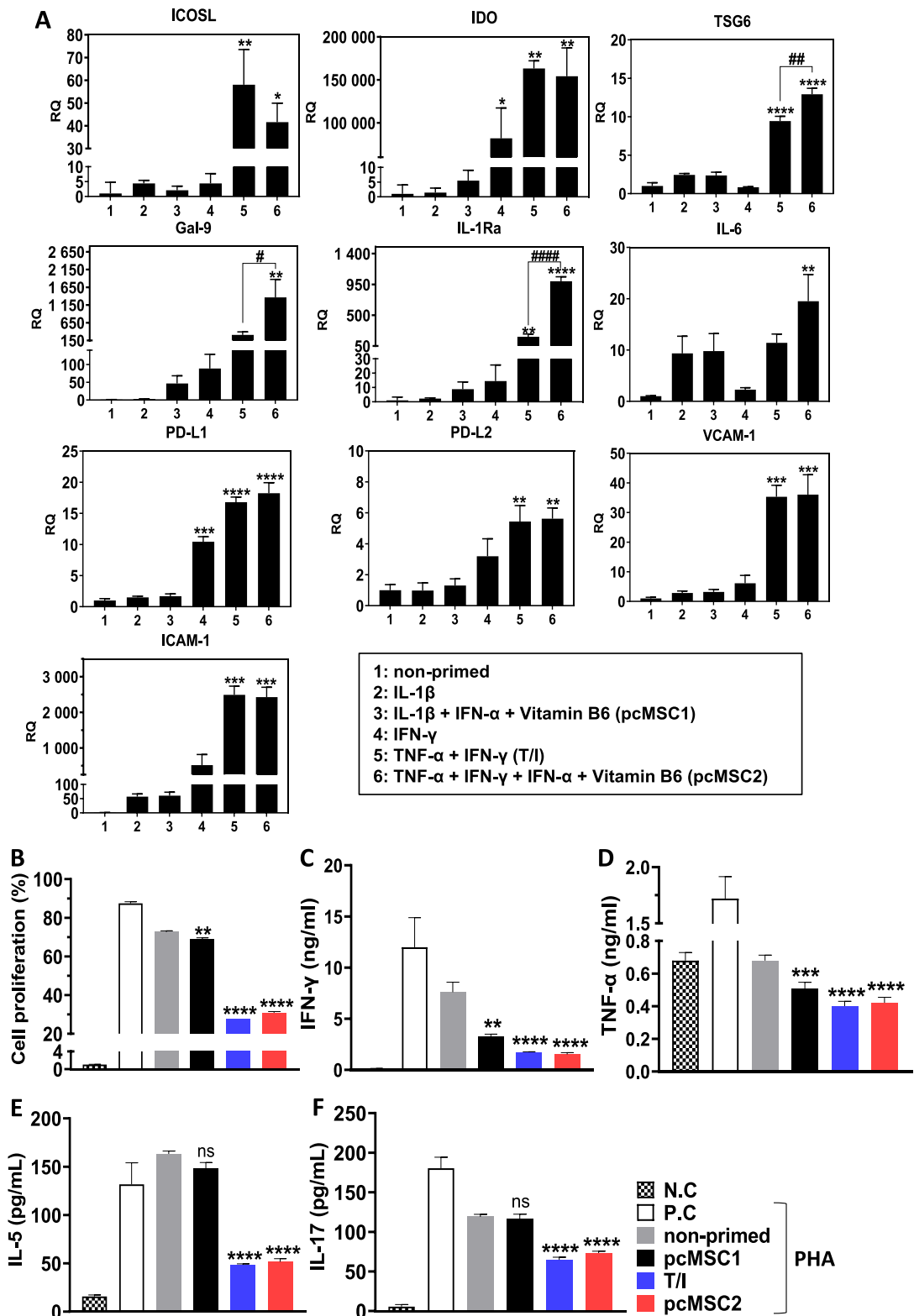
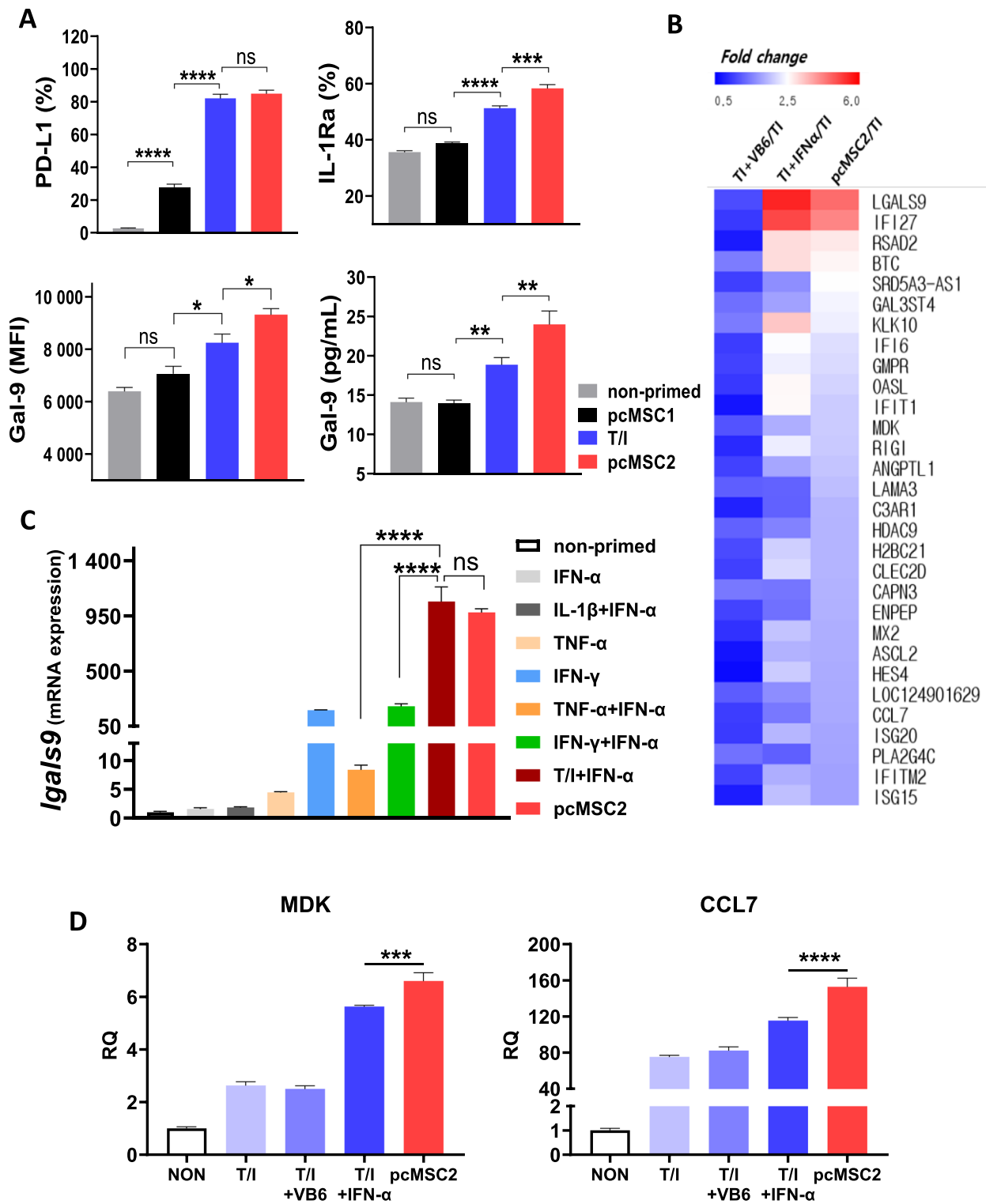


**Fig. 3** (See legend on previous page.)





material 1). The gene that showed the most significant increase in pcMSC2 compared with T/I-primed cMSCs was *LGALS9* (Gal-9), whose expression was primarily upregulated by IFN- $\alpha$ . In addition, we confirmed the mRNA expression of *LGALS9* in cMSCs using various combinations of IL-1 $\beta$ , TNF- $\alpha$ , IFN- $\gamma$ , and IFN- $\alpha$  through qRT-PCR (Fig. 4C). The results indicated that *LGALS9* mRNA expression was highest in cMSCs primed with a combination of T/I and IFN- $\alpha$ . Furthermore, we found that Vit B6, in conjunction with IFN- $\alpha$  and T/I, synergistically induced the mRNA expression of *CCL7* and *midkine* (MDK), which are involved in T-cell migration and Th1 differentiation, respectively (Fig. 4D).

#### Effects of primed cMSCs on regulatory T cells and Th17 differentiation

The effects of Gal-9 from pcMSC2 on Treg and Th17 differentiation were evaluated. The induction of FOXP3<sup>+</sup> Tregs and the secretion of IL-10 were significantly greater in the presence of pcMSC2 than in the presence of nonprimed cMSCs ( $p < 0.0001$ ) (Fig. 5A and B). Furthermore, the highest Gal-9 secretion levels were observed when CD4<sup>+</sup> T cells were cocultured with pcMSC2 (Fig. 5B). To identify the factors involved in Treg induction, we used neutralizing antibodies against PD-L1, IL-1Ra, and Gal-9. Our findings revealed that anti-Gal-9 treatment did not induce FOXP3<sup>+</sup> Tregs (Fig. 5C). These findings indicate that Gal-9 derived from pcMSC2 plays a crucial role in promoting Treg induction. Under conditions that promoted Th17 differentiation, all cMSCs exhibited a decrease in IL-17A production, with pcMSC2 demonstrating an even greater reduction in IL-17A levels than nonprimed cMSCs did ( $p < 0.0001$ ) (Fig. 5D). IL-2 inhibits the differentiation of Th17 cells. Notably, elevated IL-2 levels were observed exclusively in the pcMSC2 treatment group. These findings suggest that pcMSC2 increases IL-2 production, potentially leading to a reduction in Th17 cell differentiation. However, Gal-9 did not affect Th17 cell differentiation (Fig. 5E).

#### Induction of late apoptotic T cells by Gal-9

To investigate whether pcMSC2-mediated Gal-9 is involved in T-cell apoptosis, we stimulated PBMCs with anti-CD3 and anti-CD28 antibodies and cocultured them with pcMSC2 cells in the presence of anti-Gal-9 neutralizing antibodies. The percentage of late apoptotic cells induced by pcMSC2 was significantly greater than that induced by nonprimed cMSCs ( $p < 0.001$ ). However, when Gal-9 was neutralized with antibodies, the number of late apoptotic cells decreased to levels comparable with those with nonprimed cMSCs (Fig. 6). In conclusion, the increased secretion of Gal-9 by pcMSC2 cells further promotes T-cell apoptosis.

#### Primed cMSCs alleviate ovalbumin-induced AD in mice

Inflammation in skin lesions and serum immunoglobulin levels were analyzed. Histopathological examination revealed alleviated epidermal hypertrophy and hyperkeratosis in all cMSC-treated mice (Fig. 7A). H&E staining showed a decrease in cell infiltration in the skin of cMSC-treated mice compared with the vehicle-treated positive control mice. Notably, treatment with pcMSC2 resulted in the most significant reduction in epidermal thickness ( $p < 0.001$ ) (Figs. 7A and B). Furthermore, pcMSCs did not significantly affect dermal thickness.

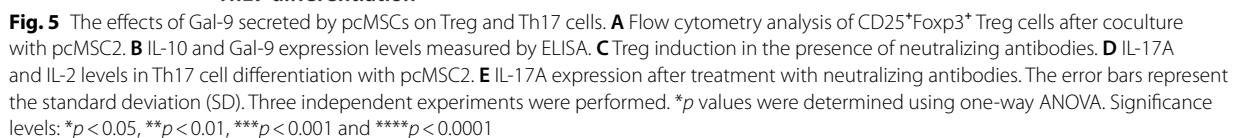
The number of mast cells decreased in all the pcMSC groups, with a more pronounced effect observed in the pcMSC2 group. Interestingly, the number of eosinophils was significantly reduced in both the pcMSC2- and T/I-primed cMSC-treated mice, with a more pronounced effect noted in the pcMSC2-treated group (Fig. 7A and C). Additionally, we observed a reduction in the expression of CLDN1, a critical component of tight junctions, in AD skin lesions. CLDN1 expression was significantly restored in both pcMSC2- and T/I-primed cMSC-treated mice, with pcMSC2 treatment resulting in the most significant restoration of CLDN1 expression (Figs. 7A and D).

Serum immunoglobulin levels were measured using ELISAs. Total IgE levels significantly decreased in the pcMSC2-treated mice ( $p < 0.01$ ). In contrast, the T/I- and pcMSC2-treated mice presented increased IgG2a levels (Fig. 7E).

Additionally, we examined the mRNA expression of Th2 cytokines and the CD8 $\alpha$  chain in skin lesions. Compared with nonprimed cMSCs, all pcMSCs presented significantly decreased IL-4 mRNA levels ( $p < 0.001$ ) (Fig. 7F). Notably, the mRNA expression levels of IL-5 and CD8 $\alpha$  were significantly reduced only by pcMSC2 (IL-5:  $p = 0.0134$ , CD8 $\alpha$ :  $p = 0.0148$ ) (Fig. 7F). These findings suggest that pcMSC2 is the most effective agent for alleviating OVA-induced AD.

#### Discussion

In this study, we observed that priming with our newly identified combination of factors—IFN- $\alpha$ , vitamin B6, and T/I—significantly promoted the immunomodulatory function of cMSCs. IFN- $\alpha$  regulates immune responses, particularly in antiviral defense and cancer protection [37, 38]. Vit B6 (or pyridoxine), a water-soluble vitamin, is a vital coenzyme in more than 150 biochemical reactions within cells. This vitamin is essential for amino acid metabolism and contributes to carbohydrate and lipid metabolism, as well as neurotransmitter synthesis. These functions render it indispensable for cellular signaling, antioxidant activity, and immune regulation [39, 40]. To evaluate whether primed cMSCs could alter their



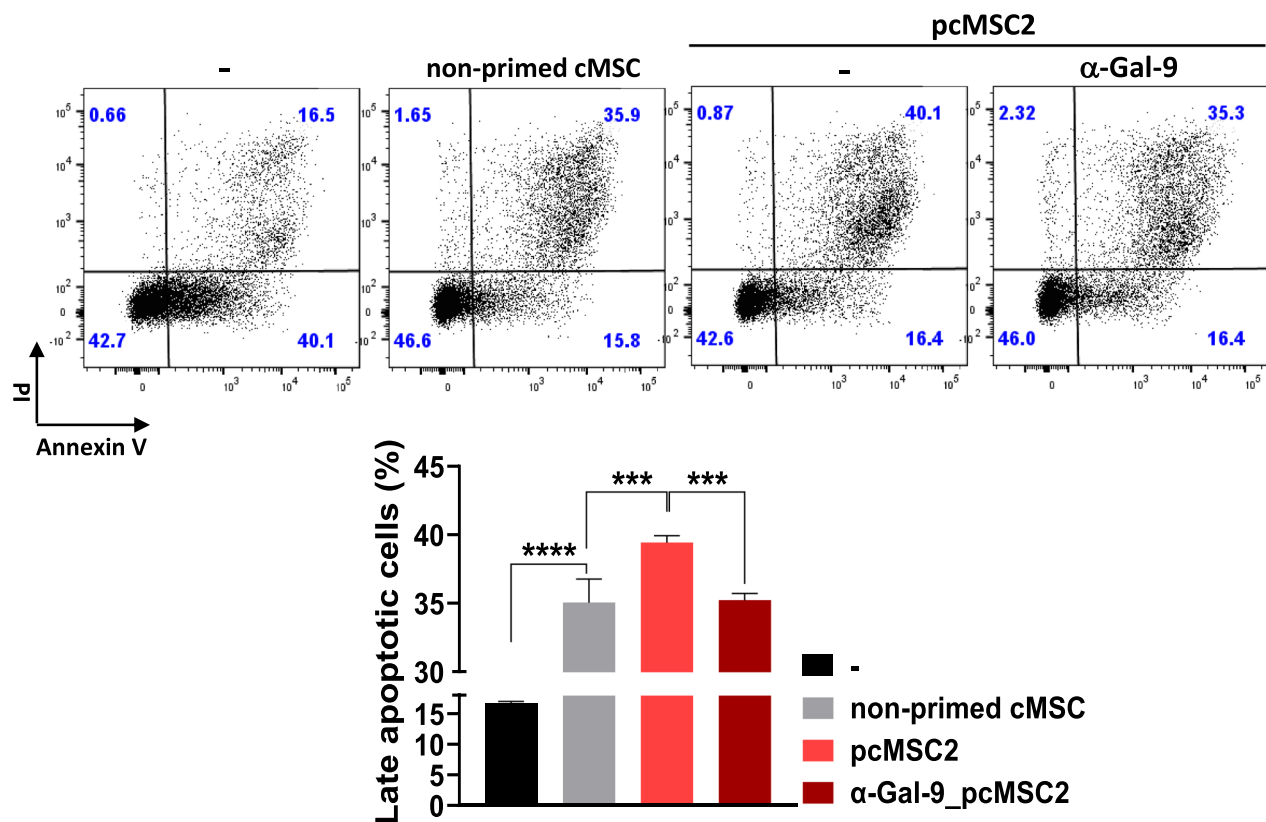


**Fig. 6** Effects of Gal-9 secreted by pcMSC2 on CD4<sup>+</sup> T-cell apoptosis. Flow cytometry analysis of late apoptotic CD4<sup>+</sup> T cells after coculture with pcMSC2 under CD3/CD28 stimulation, with or without Gal-9 neutralization. The error bars represent the standard deviation (SD). Three independent experiments were performed. \**p* values were determined using one-way ANOVA. Significance levels: \*\*\**p* < 0.001 and \*\*\*\**p* < 0.0001

(See figure on next page.)

**Fig. 7** Primed cMSCs alleviated OVA-induced AD. **A** Histological analysis of skin tissues by H&E, toluidine blue, Congo red, and IF staining for CLDN1. **B, C** Quantification of skin thickness, mast cells, and eosinophils. **D** CLDN1 expression shown as MFI per unit area. **E** Serum levels of IgE, IgG1, and IgG2a measured by ELISA. **F** Relative mRNA expression in skin lesions. Data are presented as mean ± SEM. Unpaired *t* tests were used for statistical analysis: \**p* values indicate differences from the vehicle group, #*p* values from the nonprimed group, and the comparison with T/I-primed cMSCs is shown as a numerical *p* value. Significance levels: \**p* < 0.05, \*\**p* < 0.01, \*\*\**p* < 0.001, \*\*\*\**p* < 0.0001, #*p* < 0.05, ##*p* < 0.01, ###*p* < 0.001 and ####*p* < 0.0001

fundamental properties or induce genetic mutations, we assessed the viability, morphology, and differentiation potential of pcMSC2 cells and confirmed that the essential properties of cMSCs were preserved. In addition, we examined genetic abnormality and tumorigenicity and found no evidence of such occurrences (Supplementary Fig. S4, Table S2).

We further observed that treatment with the primed pcMSCs significantly alleviated pathological changes in an AD mouse model (Fig. 7). pcMSC2 cells significantly reduced the epidermal thickness, which was increased by AD induction. In addition, pcMSC2 cells significantly decreased the infiltration of mast cells and eosinophils as well as total IgE, IL-4, and IL-5 expression. Several

studies have demonstrated that the expression of CLDN1, a critical component of tight junctions, is diminished in skin lesions affected by AD; this reduction results in compromised tight junction barrier function and subsequent epidermal inflammation. Elevating CLDN1 levels has been shown to promote barrier function and mitigate inflammation, making it a potential therapeutic target for AD [41, 42]. pcMSC2 significantly restored the CLDN1 levels, indicating that pcMSC2 promoted skin barrier function.

CD8α<sup>+</sup> T cells and CD8α<sup>+</sup> dendritic cells (DCs) play crucial roles in the induction of skin inflammation and immune responses. CD8α<sup>+</sup> T cells infiltrate AD lesions in response to allergen exposure, recruiting additional

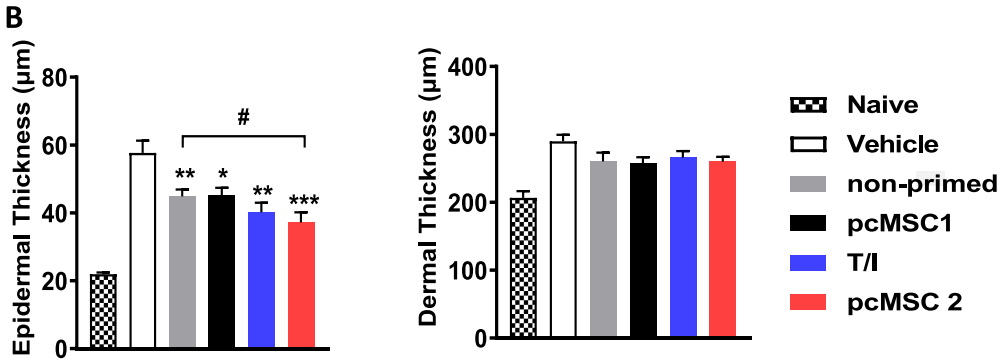
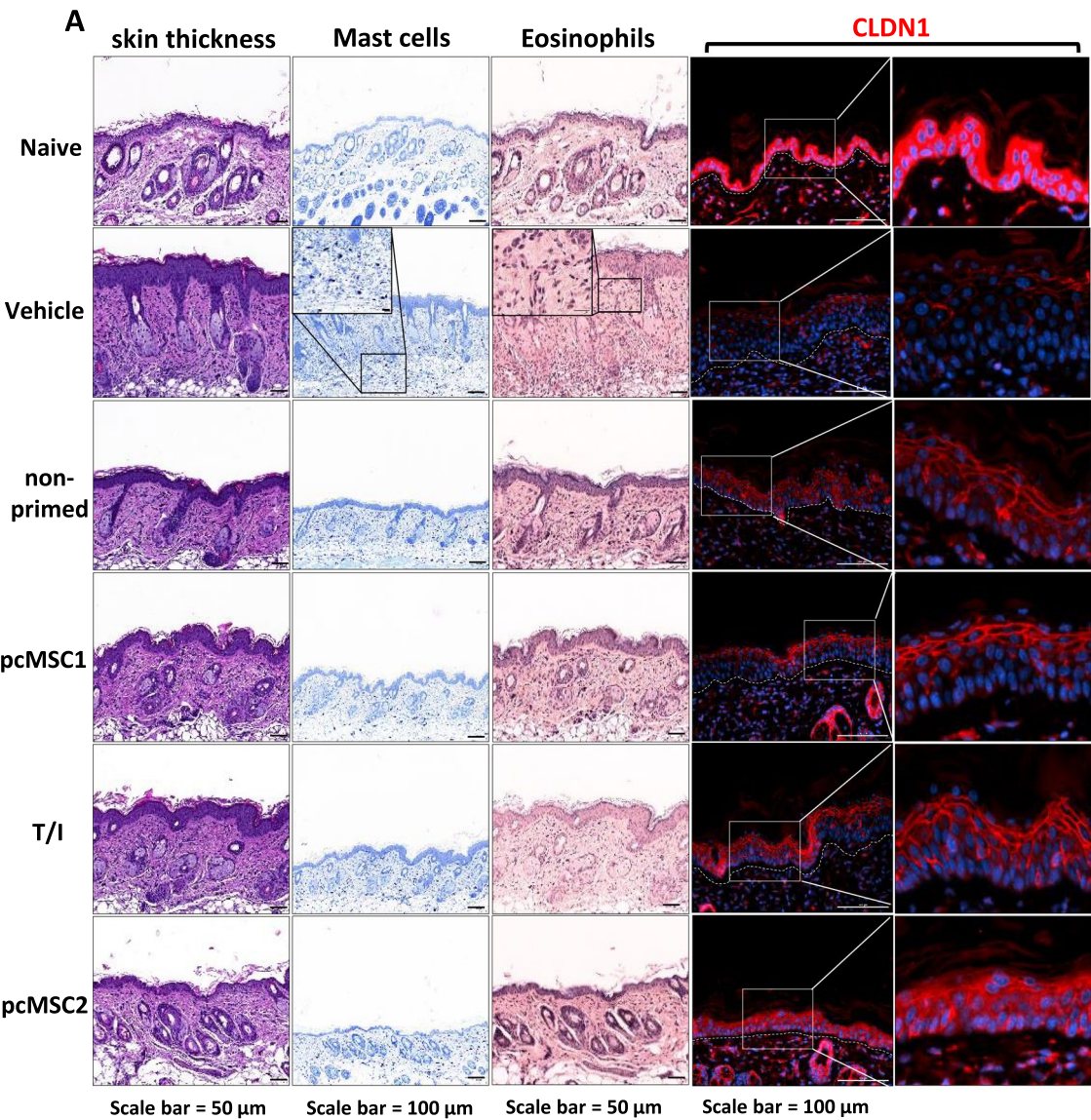


**Fig. 7** (See legend on previous page.)

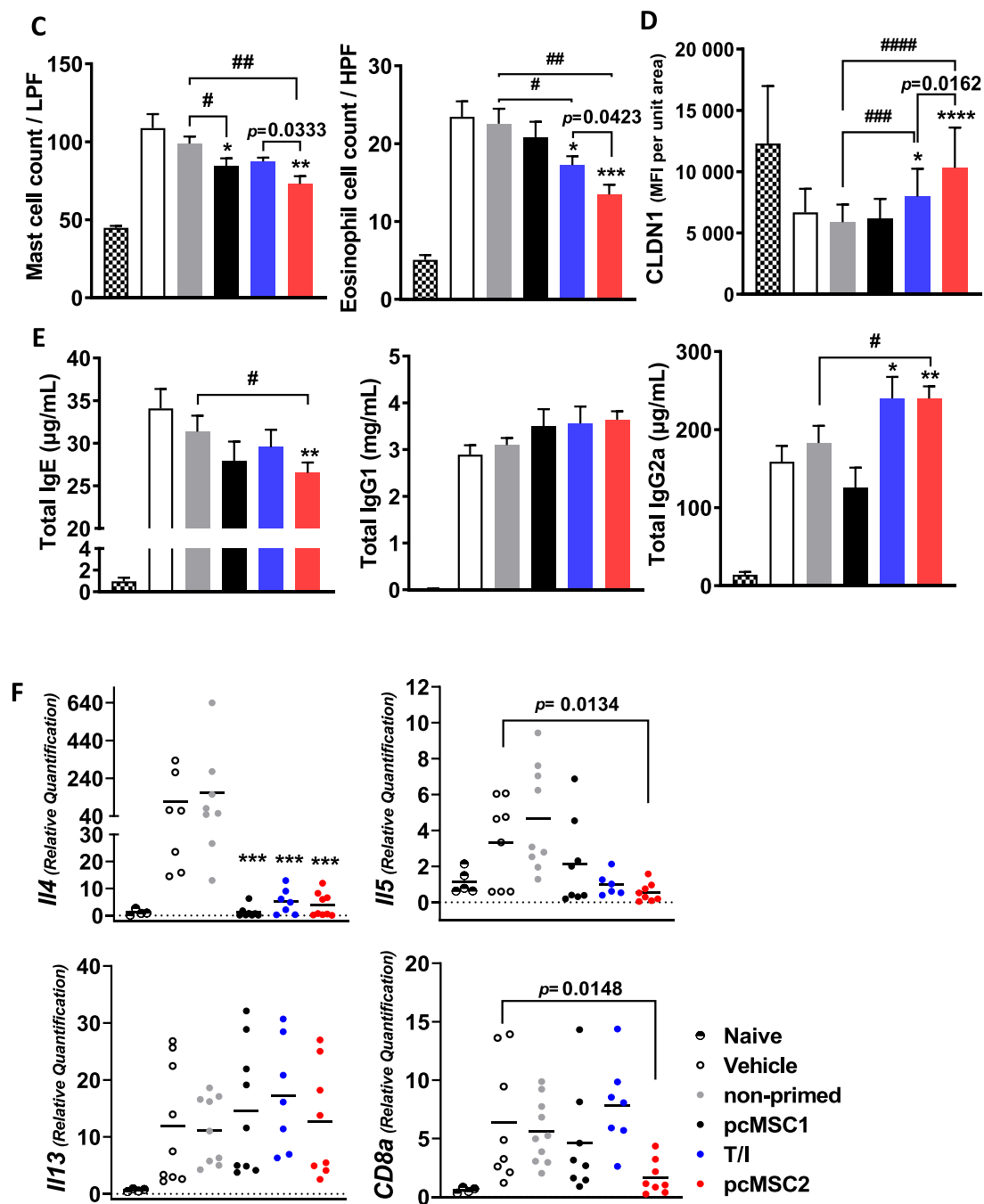


Fig. 7 continued

immune cells such as eosinophils and Th1/Th2 cells and further exacerbating skin inflammation [43, 44]. CD8 $\alpha^+$  DCs contribute to AD by presenting antigens and activating T cells within the skin [45, 46]. Notably, we observed a significant decrease in the mRNA expression of CD8 $\alpha$  in the epidermis of skins treated with

pcMSC2 (Fig. 7F), suggesting a reduction in the infiltration of CD8 $\alpha^+$  T cells or CD8 $\alpha^+$  DCs.

Furthermore, the significant reduction in eosinophil infiltration and IL-5 by pcMSC2 (Fig. 7C, F), which results in high Gal-9 expression levels, is crucial for understanding its immunomodulatory effects in AD.



Gal-9 facilitates eosinophil chemotaxis and apoptosis and is a critical factor that modulates Th2-mediated eosinophilic inflammation [47, 48].

Most importantly, Gal-9 is a crucial protein in the galectin family, known for its critical role in immune regulation, with significant implications in cancer, autoimmune diseases, and inflammatory conditions [49, 50]. Gal-9 binds to  $\beta$ -galactoside sugars and plays substantial roles in cell–cell adhesion, immune response modulation, and apoptosis. One of its critical functions is its interaction with the TIM-3 receptor, which is present in T cells and other immune cells. This interaction can induce immune tolerance and inhibit overactive immune responses [51, 52].

Previously, we demonstrated that cMSCs cocultured with PBMCs under PHA stimulation presented increased expression of Gal-9, a protein that inhibits T-cell proliferation [20]. Therefore, we screened priming factors that can induce Gal-9 expression and found that IFN- $\alpha$  and Vit B6 combined with T/I increased Gal-9 expression more than T/I alone did (Fig. 4A). Gal-9 is known to induce Treg differentiation and promote T-cell apoptosis [53–56]. We confirmed that Gal-9, which is highly expressed in pcMSC2, promotes FOXP3<sup>+</sup> Treg induction and increases the proportion of late apoptotic CD4<sup>+</sup> T cells. Although we did not identify a direct correlation between Gal-9 expression and the inhibition of Th17 differentiation, we observed that pcMSC2 significantly inhibited Th17 differentiation. One possible explanation for this phenomenon is the sustained presence of IL-2 in the pcMSC2-treated cells, which may contribute to the suppression of Th17 cells. IL-2 inhibits the expression of the critical Th17-related genes, *IL17A* and *IL17F*, through the STAT5 signaling pathway. IL-2-activated STAT5 competes with STAT3 to prevent STAT3 from activating *IL17A* expression [57, 58]. Therefore, targeting Gal-9 may be an effective strategy for identifying novel priming factors that increase therapeutic efficacy in disease treatment.

In addition to Gal-9, RNA sequencing data revealed a synergistic upregulation of multiple genes induced by the combination of IFN- $\alpha$  and Vit B6. These genes included MDK, CCL7, HDAC9, laminin alpha-3 subunit (LAMA3), and angiopoietin-like protein 1 (ANGPTL1), which play crucial roles in immune regulation. MDK is a growth factor expressed by MSCs, and its overexpression increases MSC survival and improves cardiac function in vivo [59]. Recombinant MDK promotes the in vitro differentiation of Th1 cells by activating STAT4 [60]. Therefore, MDK produced by pcMSC2 may be beneficial for treating Th2 diseases such as AD. Although CCL7, also known as monocyte chemotactic protein (MCP)-3, functions as a chemotactic factor for monocytes and

neutrophils, it also plays a crucial role in the migration of CD8<sup>+</sup> T cells within the virus-infected central nervous system (CNS) and directs MSCs to sites of inflammation [61, 62]. In our previous study, we observed that following the administration of MSCs in an OVA-induced AD mouse model, cMSCs migrated to skin lesions and the lymph nodes adjacent to these lesions [35]. Consequently, CCL7, which is mediated by pcMSC2, may facilitate the migration of MSCs and immune cells to the sites of injury, where it recruits T cells and modulates their activity.

HDAC9, LAMA3, and ANGPTL1 have been implicated in immune modulation in AD. Several studies have indicated that HDAC9 suppresses the expression of genes that regulate inflammatory responses, potentially contributing to the pathogenesis of inflammatory skin diseases, such as AD. Reduced HDAC9 expression is associated with heightened inflammatory responses in the skin, exacerbating AD symptoms [63, 64]. LAMA3 is linked to skin barrier integrity, and genetic mutations in LAMA3 are associated with skin barrier dysfunction, which can trigger inflammation. Research has demonstrated that specific mutations in LAMA3, which compromise skin integrity and promote inflammation, are more prevalent among patients with AD. These findings suggest that LAMA3 is critical in AD development and presents a potential therapeutic strategy for restoring skin barrier function [65]. In addition, ANGPTL1 is recognized for its anti-inflammatory and antiangiogenic properties and may operate within pathways related to skin inflammation and immune responses. Because of its role in alleviating tissue inflammation, ANGPTL1 is a promising factor that may influence chronic inflammatory diseases, such as AD [66, 67].

Future studies should investigate the mechanisms through which pcMSC2 suppresses Th17 differentiation and the roles of other factors that are highly expressed by pcMSC2, such as MDK, CCL7, HDAC9, LAMA3, and ANGPTL1, in the treatment of AD. Furthermore, unlike other pcMSCs, pcMSC2 strongly suppresses CD8 $\alpha$  mRNA expression. However, this study did not clarify which specific factor in pcMSC2 is responsible for this effect or the underlying mechanism. Further research is needed to investigate this aspect in detail.

## Conclusions

In conclusion, by targeting Gal-9, we identified a novel combination of priming factors—IFN- $\alpha$  and vitamin B6—in combination with TNF- $\alpha$  and IFN- $\gamma$ . This approach transforms cMSCs with low immunomodulatory capacity into cMSCs with increased immunomodulatory abilities. Primed cMSCs alleviated AD by restoring CLDN1 expression and inhibiting the infiltration of mast cells and

eosinophils, thereby strengthening skin barrier function. Additionally, pcMSC2 reduced CD8 $\alpha$  expression in the skin while modulating the balance of Th1/Th2 responses. Given the challenges associated with identifying suitable stem cells for therapeutic applications, priming factors that target Gal-9 may significantly increase the efficacy of stem cell therapies.

#### Abbreviations

cMSCs	Clonal mesenchymal stem cells
pcMSCs	Primed-cMSCs
T/I	TNF- $\alpha$ and IFN- $\gamma$
pcMSC1	CMSCs primed with IL-1 $\beta$ , IFN- $\alpha$ , and vitamin B6
pcMSC2	CMSCs primed with T/I, IFN- $\alpha$ , and vitamin B6
N.C	Negative control
P.C	Positive control
Vit B6	Vitamin B6
Gal-9	Galectin-9
AD	Atopic dermatitis
Treg	Regulatory T cells
PDL	Population doubling level
PDT	Population doubling time

#### Supplementary Information

The online version contains supplementary material available at <https://doi.org/10.1186/s13287-025-04394-3>.

Additional file1 (XLSX 21 KB)

Additional file2 (PDF 708 KB)

#### Acknowledgements

Not applicable. The authors declare that they have not used Artificial Intelligence in this study.

#### Author contributions

JHN, JHM, and MSJ designed the experimental strategy. JHN, JHM, BC, GHK, YK, SYP, and THK performed the experiments. DS, YSJ, SNK, YKC, and MSJ supervised the project and interpreted the results. JHN and MSJ wrote the manuscript. All authors reviewed and approved the manuscript.

#### Funding

This research was supported by grants from the National Research Foundation of Korea (NRF-2022R1A2C1010354) and the Korean Fund for Regenerative Medicine (KFRM) grant funded by the Korean government (the Ministry of Science and ICT, the Ministry of Health & Welfare). (KFRM-24B0101L1).

#### Data availability

The authors confirm that the data supporting this study's findings are available within the article and its supplementary materials. The raw sequence data for analysis are available in supplementary material 1. Any other relevant materials used and/or analyzed during the current study are available from the corresponding author upon reasonable request.

#### Declarations

##### Ethics approval and consent to participate

This study includes samples from both humans and animals. The isolation of human cMSC from bone marrow samples was approved by three institutions: 1. The study titled "Bone Marrow Donation for Harvesting, Clinical Trial Researching, and Culturing of Stem Cell Therapeutics Bone Marrow-Derived Adult Stem Cells from Healthy Donors" received approval from the IRB of the Catholic University of Korea, Seoul St. Mary's Hospital, with the approval number IRB No. KC15CSSE0336, dated December 14, 2014. 2. The study titled "Bone Marrow Donation for Harvesting and Culturing Bone Marrow-Derived Adult Stem Cells from Healthy Donors" was approved by the IRB of Inha University

Hospital, with the approval number IRB No. 10–51, dated October 11, 2010. 3. The study titled "Clinical Grade Bone Marrow Collection for Clinical Research and/or Future Manufacturing of Human Cell Therapy Products" was approved by AllCells (Alameda, CA, USA), with the approval number IRB No. 949–542–3882, dated December 14, 2020. The use of PBMC from healthy donors has been approved. The study titled "Blood Donation from Healthy Donors for Analyzing the Immune Mechanism of Adult Stem Cells" received approval from the IRB of Inha University Hospital, with approval number IRB No. 2014–01–082–019, dated November 14, 2022. Written informed consent was obtained from all study participants. The "Efficacy Evaluation of Cell Therapy for the Treatment of Atopic Dermatitis" study received approval from the IACUC of Gachon University for the mouse experiments. The approval number is IACUC No. LCDI-2023–0054, dated June 14, 2023.

##### Consent for publication

All authors gave consent for publication.

##### Competing interests

The authors have declared no competing interests.

Received: 6 January 2025 Accepted: 14 May 2025

Published online: 30 May 2025

#### References

- Huang Y, Wu Q, Tam PKH. Immunomodulatory mechanisms of mesenchymal stem cells and their potential clinical applications. *Int J Mol Sci*. 2022;23(17):10023. <https://doi.org/10.3390/ijms231710023>.
- Yang G, Fan X, Liu Y, Jie P, Mazhar M, Liu Y, et al. Immunomodulatory mechanisms and therapeutic potential of mesenchymal stem cells. *Stem Cell Rev Rep*. 2023;19(5):1214–31.
- Sharan J, Barmada A, Band N, Liebman E, Prodromos C. First report in a human of successful treatment of asthma with mesenchymal stem cells: a case report with review of literature. *Curr Stem Cell Res Ther*. 2023;18(7):1026–9.
- MacLoughlin R. Advancing mesenchymal stem cell therapy for asthma towards clinical translation. *Ann Transl Med*. 2022;10(20):1083.
- Dalal J, Gandy K, Domen J. Role of mesenchymal stem cell therapy in Crohn's disease. *Pediatr Res*. 2012;71(4 Pt 2):445–51.
- Daltro SR, Meira CS, Santos IP, Ribeiro dos Santos R, Soares MB. Mesenchymal stem cells and atopic dermatitis: a review. *Front Cell Develop Biol*. 2020;8:326.
- Jeon MS, Yi TG, Lim HJ, Moon SH, Lee MH, Kang JS, et al. Characterization of mouse clonal mesenchymal stem cell lines established by subfractionation culturing method. *World J Stem Cells*. 2011;3(8):70–82.
- Song SU, Kim CS, Yoon SP, Kim SK, Lee MH, Kang JS, et al. Variations of clonal marrow stem cell lines established from human bone marrow in surface epitopes, differentiation potential, gene expression, and cytokine secretion. *Stem Cells Dev*. 2008;17(3):451–61.
- Dunn CM, Kameishi S, Grainger DW, Okano T. Strategies to address mesenchymal stem/stromal cell heterogeneity in immunomodulatory profiles to improve cell-based therapies. *Acta Biomater*. 2021;133:114–25.
- Yoo HS, Yi T, Cho YK, Kim WC, Song SU, Jeon MS. Mesenchymal stem cell lines isolated by different isolation methods show variations in the regulation of graft-versus-host disease. *Immune Netw*. 2013;13(4):133–40.
- Kavanagh DP, Robinson J, Kalia N. Mesenchymal stem cell priming: fine-tuning adhesion and function. *Stem Cell Rev Rep*. 2014;10(4):587–99.
- Herger N, Heggli I, Mengis T, Devan J, Arpesella L, Brunner F, et al. Impacts of priming on distinct immunosuppressive mechanisms of mesenchymal stromal cells under translationally relevant conditions. *Stem Cell Res Ther*. 2024;15(1):65.
- Noronha NC, Mizukami A, Caliri-Oliveira C, Cominal JG, Rocha JLM, Covas DT, et al. Priming approaches to improve the efficacy of mesenchymal stromal cell-based therapies. *Stem Cell Res Ther*. 2019;10(1):131.
- Miceli V. Use of priming strategies to advance the clinical application of mesenchymal stromal/stem cell-based therapy. *World J Stem Cells*. 2024;16(1):7–18.
- Lopez-Garcia L, Castro-Manrreza ME. TNF-alpha and IFN-gamma participate in improving the immunoregulatory capacity of mesenchymal

- stem/stromal cells: importance of cell-cell contact and extracellular vesicles. *Int J Mol Sci.* 2021;22(17):9531.
16. Francois M, Romieu-Mourez R, Li M, Galipeau J. Human MSC suppression correlates with cytokine induction of indoleamine 2,3-dioxygenase and bystander M2 macrophage differentiation. *Mol Ther.* 2012;20(1):187–95.
17. de Pedro M<sup>A</sup>, Gómez-Serrano M, Marinaro F, López E, Pulido M, Preusser C, et al. IFN- $\gamma$  and TNF- $\alpha$  as a priming strategy to enhance the immunomodulatory capacity of secretomes from menstrual blood-derived stromal cells. *Int J Mol Sci.* 2021;22(22):12177.
18. Harting MT, Srivastava AK, Zhaorigetu S, Bair H, Prabhakara KS, Toledano Furman NE, et al. Inflammation-stimulated mesenchymal stromal cell-derived extracellular vesicles attenuate inflammation. *Stem Cells.* 2018;36(1):79–90.
19. Montesinos JJ, Lopez-Garcia L, Cortes-Morales VA, Arriaga-Pizano L, Valle-Rios R, Fajardo-Orduna GR, et al. Human bone marrow mesenchymal stem/stromal cells exposed to an inflammatory environment increase the expression of ICAM-1 and release microvesicles enriched in this adhesive molecule: analysis of the participation of TNF- $\alpha$  and IFN- $\gamma$ . *J Immunol Res.* 2020;2020:8839625.
20. Kim SN, Lee HJ, Jeon MS, Yi T, Song SU. Galectin-9 is involved in immunosuppression mediated by human bone marrow-derived clonal mesenchymal stem cells. *Immune Netw.* 2015;15(5):241–51.
21. English K, Barry FP, Field-Corbett CP, Mahon BP. IFN- $\gamma$  and TNF- $\alpha$  differentially regulate immunomodulation by murine mesenchymal stem cells. *Immunol Lett.* 2007;110(2):91–100.
22. Pestka S. The interferons: 50 years after their discovery, there is much more to learn. *J Biol Chem.* 2007;282(28):20047–51.
23. Pestka S, Langer JA, Zoon KC, Samuel CE. Interferons and their actions. *Annu Rev Biochem.* 1987;56:727–77.
24. Borden EC. Interferons: pleiotropic cellular modulators. *Clin Immunol Immun.* 1992;62(1 Pt 2):S18–24.
25. Zhang T, Wang Y, Li Q, Lin L, Xu C, Xue Y, et al. Mesenchymal stromal cells equipped by IFN $\alpha$  empower T cells with potent anti-tumor immunity. *Oncogene.* 2022;41(13):1866–81.
26. Liu S, Liu F, Zhou Y, Jin B, Sun Q, Guo S. Immunosuppressive property of MSCs mediated by cell surface receptors. *Front Immunol.* 2020;11:1076.
27. Panahi M, Rahimi B, Rahimi G, Yew Low T, Saraygord-Afshari N, Alizadeh E. Cytoprotective effects of antioxidant supplementation on mesenchymal stem cell therapy. *J Cell Physiol.* 2020;235(10):6462–95.
28. Yang M, Teng S, Ma C, Yu Y, Wang P, Yi C. Ascorbic acid inhibits senescence in mesenchymal stem cells through ROS and AKT/mTOR signaling. *Cyto-technology.* 2018;70(5):1301–13.
29. Kim JH, Kim WK, Sung YK, Kwack MH, Song SY, Choi JS, et al. The molecular mechanism underlying the proliferating and preconditioning effect of vitamin C on adipose-derived stem cells. *Stem Cells Dev.* 2014;23(12):1364–76.
30. Li C, Huang J, Zhu H, Shi Q, Li D, Ju X. Pyridoxal-5'-phosphate promotes immunomodulatory function of adipose-derived mesenchymal stem cells through indoleamine 2,3-dioxygenase-1 and TLR4/NF- $\kappa$ B pathway. *Stem Cells Int.* 2019;2019:3121246.
31. Lee HJ, Kim SN, Jeon MS, Yi T, Song SU. ICOSL expression in human bone marrow-derived mesenchymal stem cells promotes induction of regulatory T cells. *Sci Rep.* 2017;7:44486.
32. Manel N, Unutmaz D, Littman DR. The differentiation of human T(H)-17 cells requires transforming growth factor- $\beta$  and induction of the nuclear receptor ROR $\gamma$ mat. *Nat Immunol.* 2008;9(6):641–9.
33. Romagnani S, Maggi E, Liotta F, Cosmi L, Annunziato F. Properties and origin of human Th17 cells. *Mol Immunol.* 2009;47(1):3–7.
34. Jin H, He R, Oyoshi M, Geha RS. Animal models of atopic dermatitis. *J Invest Dermatol.* 2009;129(1):31–40.
35. Na K, Yoo HS, Zhang YX, Choi MS, Lee K, Yi TG, et al. Bone marrow-derived clonal mesenchymal stem cells inhibit ovalbumin-induced atopic dermatitis. *Cell Death Dis.* 2014;5(7):e1345.
36. Na K, Lkhagva-Yondon E, Kim M, Lim YR, Shin E, Lee CK, et al. Oral treatment with Aloe polysaccharide ameliorates ovalbumin-induced atopic dermatitis by restoring tight junctions in skin. *Scand J Immunol.* 2020;91(3):e12856.
37. Sengupta P, Chattopadhyay S. Interferons in viral infections. *Viruses.* 2024;16(3):451.
38. Teijaro JR. Type I interferons in viral control and immune regulation. *Curr Opin Virol.* 2016;16:31–40.
39. Parra M, Stahl S, Hellmann H. Vitamin B(6) and Its role in cell metabolism and physiology. *Cells.* 2018;7(7):84.
40. Mikkelsen K, Dargahi N, Fraser S, Apostolopoulos V. High-dose vitamin B6 (Pyridoxine) displays strong anti-inflammatory properties in lipopolysaccharide-stimulated monocytes. *Biomedicines.* 2023;11(9):2578.
41. Bergmann S, von Buenau B, Vidal YSS, Haftek M, Wladykowski E, Houdek P, et al. Claudin-1 decrease impacts epidermal barrier function in atopic dermatitis lesions dose-dependently. *Sci Rep.* 2020;10(1):2024.
42. Tokumasu R, Yamaga K, Yamazaki Y, Murota H, Suzuki K, Tamura A, et al. Dose-dependent role of claudin-1 in vivo in orchestrating features of atopic dermatitis. *Proc Natl Acad Sci U S A.* 2016;113(28):E4061–8.
43. Hennino A, Vocanson M, Toussaint Y, Rodet K, Benetiere J, Schmitt AM, et al. Skin-infiltrating CD8 $^{+}$  T cells initiate atopic dermatitis lesions. *J Immunol.* 2007;178(9):5571–7.
44. Savinko T, Lauerma A, Lehtimäki S, Gombert M, Majuri ML, Fyhrquist-Vanni N, et al. Topical superantigen exposure induces epidermal accumulation of CD8 $^{+}$  T cells, a mixed Th1/Th2-type dermatitis and vigorous production of IgE antibodies in the murine model of atopic dermatitis. *J Immunol.* 2005;175(12):8320–6.
45. Vella JL, Molodtsov A, Angeles CV, Branchini BR, Turk MJ, Huang YH. Dendritic cells maintain anti-tumor immunity by positioning CD8 skin-resident memory T cells. *Life Sci Alliance.* 2021;4(10):e202101056. <https://doi.org/10.26508/lsa.202101056>.
46. Gombert M, Dieu-Nosjean MC, Winterberg F, Bunemann E, Kubitz RC, Da Cunha L, et al. CCL1-CCR8 interactions: an axis mediating the recruitment of T cells and Langerhans-type dendritic cells to sites of atopic skin inflammation. *J Immunol.* 2005;174(8):5082–91.
47. Katoh S, Nobumoto A, Matsumoto N, Matsumoto K, Ehara N, Niki T, et al. Involvement of galectin-9 in lung eosinophilia in patients with eosinophilic pneumonia. *Int Arch Allergy Immunol.* 2010;153(3):294–302.
48. Katoh S, Oomizu S, Niki T, Shimizu H, Obase Y, Korenaga M, et al. Possible regulatory role of galectin-9 on Ascaris suum-induced eosinophilic lung inflammation in mice. *Int Arch Allergy Immunol.* 2012;158(Suppl 1):58–65.
49. Zhao Y, Yu D, Wang H, Jin W, Li X, Hu Y, et al. Galectin-9 Mediates the therapeutic effect of mesenchymal stem cells on experimental Endotoxemia. *Front Cell Dev Biol.* 2022;10:700702.
50. Ungerer C, Quade-Lyssy P, Radeke HH, Henschler R, Konigs C, Kohl U, et al. Galectin-9 is a suppressor of T and B cells and predicts the immune modulatory potential of mesenchymal stromal cell preparations. *Stem Cells Dev.* 2014;23(7):755–66.
51. John S, Mishra R. Galectin-9: From cell biology to complex disease dynamics. *J Biosci.* 2016;41(3):507–34.
52. Zhang M, Liu C, Li Y, Li H, Zhang W, Liu J, et al. Galectin-9 in cancer therapy: from immune checkpoint ligand to promising therapeutic target. *Front Cell Dev Biol.* 2023;11:1332205.
53. Mansour AA, Raucci F, Saviano A, Tull S, Maione F, Iqbal AJ. Galectin-9 regulates monosodium urate crystal-induced gouty inflammation through the modulation of Treg/Th17 Ratio. *Front Immunol.* 2021;12:762016.
54. Mengshol JA, Golden-Mason L, Arikawa T, Smith M, Niki T, McWilliams R, et al. A crucial role for Kupffer cell-derived galectin-9 in regulation of T cell immunity in hepatitis C infection. *PLoS ONE.* 2010;5(3):e9504.
55. Kashio Y, Nakamura K, Abedin MJ, Seki M, Nishi N, Yoshida N, et al. Galectin-9 induces apoptosis through the calcium-calpain-caspase-1 pathway. *J Immunol.* 2003;170(7):3631–6.
56. Sakai K, Kawata E, Ashihara E, Nakagawa Y, Yamauchi A, Yao H, et al. Galectin-9 ameliorates acute GVH disease through the induction of T-cell apoptosis. *Eur J Immunol.* 2011;41(1):67–75.
57. Laurence A, Tato CM, Davidson TS, Kanno Y, Chen Z, Yao Z, et al. Interleukin-2 signaling via STAT5 constrains T helper 17 cell generation. *Immunity.* 2007;26(3):371–81.
58. Luo J, Ming B, Zhang C, Deng X, Li P, Wei Z, et al. IL-2 Inhibition of Th17 generation rather than induction of treg cells is impaired in primary sjogren's syndrome patients. *Front Immunol.* 2018;9:1755.
59. Zhao SL, Zhang YJ, Li MH, Zhang XL, Chen SL. Mesenchymal stem cells with overexpression of midkine enhance cell survival and attenuate cardiac dysfunction in a rat model of myocardial infarction. *Stem Cell Res Ther.* 2014;5(2):37.
60. Masuda T, Maeda K, Sato W, Kosugi T, Sato Y, Kojima H, et al. Growth factor midkine promotes T-cell activation through nuclear factor of activated T

- cells Signaling and Th1 cell differentiation in lupus nephritis. *Am J Pathol.* 2017;187(4):740–51.
61. Bardina SV, Michlmayr D, Hoffman KW, Obara CJ, Sum J, Charo IF, et al. Differential roles of chemokines CCL2 and CCL7 in monocytoysis and leukocyte migration during west Nile virus infection. *J Immunol.* 2015;195(9):4306–18.
62. Schenk S, Mal N, Finan A, Zhang M, Kiedrowski M, Popovic Z, et al. Monocyte chemotactic protein-3 is a myocardial mesenchymal stem cell homing factor. *Stem Cells.* 2007;25(1):245–51.
63. Sawada Y, Nakatsuji T, Dokoshi T, Kulkarni NN, Liggins MC, Sen G, et al. Cutaneous innate immune tolerance is mediated by epigenetic control of MAP2K3 by HDAC8/9. *Sci Immunol.* 2021. <https://doi.org/10.1126/sciimmunol.abe1935>.
64. Sawada Y, Gallo RL. Role of epigenetics in the regulation of immune functions of the skin. *J Invest Dermatol.* 2021;141(5):1157–66.
65. Stemmler S, Parwez Q, Petrasch-Parwez E, Epplen JT, Hoffjan S. Association of variation in the LAMA3 gene, encoding the alpha-chain of laminin 5, with atopic dermatitis in a German case-control cohort. *BMC Dermatol.* 2014;14:17.
66. Santulli G. Angiopoietin-like proteins: a comprehensive look. *Front Endocrinol (Lausanne).* 2014;5:4.
67. Costa RA, Cardoso JC, Power DM. Evolution of the angiopoietin-like gene family in teleosts and their role in skin regeneration. *BMC Evol Biol.* 2017;17(1):14.

## Publisher's Note

Springer Nature remains neutral with regard to jurisdictional claims in published maps and institutional affiliations.